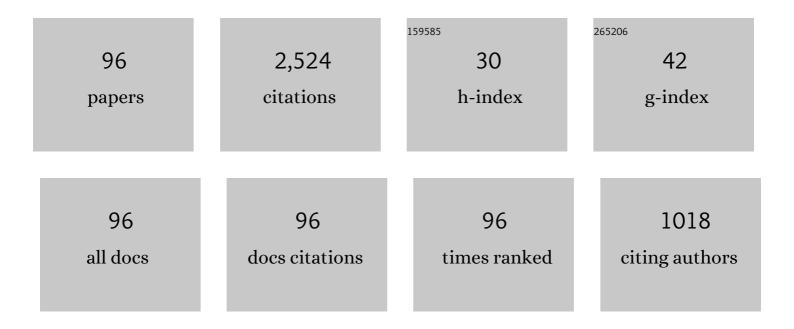
List of Publications by Year in descending order

Source: https://exaly.com/author-pdf/2138596/publications.pdf Version: 2024-02-01



SHENCLONC

#	Article	IF	CITATIONS
1	Effect of nitrogen on high temperature oxidation behavior of AlN-doped gradient coating. Corrosion Science, 2022, 199, 110155.	6.6	5
2	Effect of Al and Cr on the oxidation behavior of nanocrystalline coatings at 1050°C. Corrosion Science, 2022, 200, 110191.	6.6	14
3	Enamel coating for protection of the 316 stainless steel against tribo-corrosion in molten zinc alloy at 460 ŰC. Journal of Materials Science and Technology, 2021, 65, 126-136.	10.7	11
4	Improving oxidation resistance of <sup>î</sup> ³-TiAl based alloy by depositing TiAlSiN coating: Effects of silicon. Corrosion Science, 2021, 179, 109151.	6.6	27
5	Oxidation behavior of a nanocrystalline coating with low Ta content at high temperature. Corrosion Science, 2021, 180, 109182.	6.6	25
6	Oxidation mechanism of Ni+CrAlYNO nanocomposite coating enhanced by a NiCrAlY buffer layer. Corrosion Science, 2021, 180, 109184.	6.6	10
7	Effect of γ′ Phase Elements on Oxidation Behavior of Nanocrystalline Coatings at 1050 °C. Materials, 2021, 14, 202.	2.9	6
8	High vacuum arc ion plating Cr films: Self-ion bombarding effect and oxidation behavior. Corrosion Science, 2021, 187, 109476.	6.6	12
9	Improved oxidation resistance of γ-TiAl intermetallics by sputtered Ni+CrAlYHfSiN composite coating. Corrosion Science, 2021, 187, 109510.	6.6	16
10	Corrosion of the WC-12Co and enamel coatings in liquid Zn-55Al alloy at 640 °C. Corrosion Science, 2021, 188, 109559.	6.6	3
11	Improving the oxidation behavior of low expansion Ni + CrAlYNO coating systems by regulating the oxygen content. Corrosion Science, 2021, 189, 109582.	6.6	1
12	Thermal shock and self-healing behavior of the enamel composite coatings with addition of various nanoparticles at temperatures of 700 and 800 ŰC. Corrosion Science, 2021, 191, 109747.	6.6	12
13	Temporary enamel coatings for oxidation protection of Ti–6Al–4V at its hot working temperature of 1200â€ <sup>–</sup> °C. Journal of Alloys and Compounds, 2020, 815, 152295.	5.5	7
14	Effect of nitrogen content on the phase transformation of alumina scale on a nanocrystalline NiCrAlYSiHfN/AlN multilayer coating. Corrosion Science, 2020, 165, 108396.	6.6	12
15	Oxidation and corrosion protection of ZG12Cr9Mo1Co1NiVNbNB (CB2) ferritic stainless steel by inorganic composite coatings at 650†°C. Corrosion Science, 2020, 177, 109000.	6.6	9
16	Thermal shock and sulfuric acid corrosion behavior of enamel–nanoâ€Ni composite/enamel–nanoâ€nickel composite coating. International Journal of Applied Glass Science, 2020, 11, 784-795.	2.0	3
17	Effects of oxygen incorporation in low expansion Ni+CrAlYN nanocomposite coatings on the oxidation behavior. Corrosion Science, 2020, 167, 108550.	6.6	6
18	Oxidation behavior of Al/Y co-modified nanocrystalline coatings with different Al content on a nickel-based single-crystal superalloy. Corrosion Science, 2020, 170, 108700.	6.6	23

#	Article	IF	CITATIONS
19	Crystallization and wear behavior of SiO2-Al2O3-ZrO2-Ba(Sr, Ca)O glass-ceramics added with Cr2O3 by different methods. Ceramics International, 2019, 45, 22617-22624.	4.8	10
20	Low inter-diffusivity γ'-base bondcoats for single crystal superalloy René N5. â…j: Cyclic oxidation behavior at 1100 úC. Corrosion Science, 2019, 159, 108127.	6.6	9
21	Effect of Ti on the microstructure change and oxidation behavior of Ni+CrAlYHfSiN composite coatings. Corrosion Science, 2019, 150, 54-63.	6.6	5
22	Preparation and Oxidation Performance of a NiCoCrAlYSiHf + NiAl Composite Coating Deposited by Arc Ion Plating and Magnetron Sputtering Techniques. Journal of Materials Engineering and Performance, 2019, 28, 1019-1029.	2.5	7
23	Oxidation mechanism of a nanocrystalline NiCrAlYSiHfN/AlN multilayer coating. Corrosion Science, 2019, 156, 71-83.	6.6	10
24	Corrosion of SiO2–B2O3–Al2O3–CaF2-R2O (R=Na and K) enamels with different content of ZrO2 in H2SO4 and NaOH solutions. Ceramics International, 2019, 45, 14958-14967.	4.8	10
25	Benefits of Zr addition to oxidation resistance of a single-phase (Ni,Pt)Al coating at 1373 K. Journal of Materials Science and Technology, 2019, 35, 1334-1344.	10.7	44
26	Breakaway oxidation of a low-Al content nanocrystalline coating at 1000â€ <sup>~</sup> °C. Surface and Coatings Technology, 2019, 358, 958-967.	4.8	16
27	Corrosion of enamel with and without CaF2 in molten aluminum at 750 °C. Corrosion Science, 2019, 148, 228-236.	6.6	17
28	Isothermal oxidation behavior and microstructure change of a gradient low-expansion coating for superalloys. Corrosion Science, 2019, 147, 182-191.	6.6	11
29	Low inter-diffusivity γ'-base bondcoats for single crystal superalloy René N5. I: Primary study of microstructures and oxidation behaviors at 1100 ºC. Corrosion Science, 2019, 147, 299-312.	6.6	14
30	Stoichiometry and tribological behavior of thick Ta(N) coatings produced by direct current magnetron sputtering (DCMS). Applied Surface Science, 2018, 427, 1071-1079.	6.1	18
31	Ru-induced microstructural change in ion-plated TiN coating and its tribological properties. Surface and Coatings Technology, 2018, 354, 175-183.	4.8	19
32	Oxidation behavior of a glass-based composite coating with a low expansion cermet bond-coat and an AlN diffusion barrier on K417G superalloy. Corrosion Science, 2018, 145, 283-294.	6.6	10
33	Cyclic oxidation behavior of a multilayer composite coating for single-crystal superalloys. Corrosion Science, 2018, 145, 26-34.	6.6	15
34	Self-ion bombarded Cr films: Crystallographic orientation and oxidation behaviour. Corrosion Science, 2018, 143, 212-220.	6.6	17
35	Nanocrystalline, Enamel and Composite Coatings for Superalloys. Advances in Chemical and Materials Engineering Book Series, 2018, , 160-186.	0.3	1
36	A magnetron sputtered microcrystalline β-NiAl coating for SC superalloys. Part II. Effects of a NiCrO diffusion barrier on oxidation behavior at 1100 °C. Applied Surface Science, 2017, 407, 485-494.	6.1	37

#	Article	IF	CITATIONS
37	Hot corrosion of arc ion plating NiCrAlY and sputtered nanocrystalline coatings on a nickel-based single-crystal superalloy. Corrosion Science, 2017, 123, 27-39.	6.6	64
38	Interfacial microstructure evolution of glassâ€based coating on IC10 superalloy with a Ni <sub>3</sub> Al bondâ€coat at 1050°C. Journal of the American Ceramic Society, 2017, 100, 3451-3466.	3.8	3
39	Oxidation behavior of NiCrAlY coatings prepared by arc ion plating using various substrate biases: Effects of chemical composition and thickness of the coatings. Corrosion Science, 2017, 126, 317-323.	6.6	38
40	Diffusion of Ta and its influence on oxidation behavior of nanocrystalline coatings with different Ta, Y and Al contents. Corrosion Science, 2017, 126, 344-355.	6.6	43
41	Effect of YSZ-incorporated glass-based composite coating on oxidation behavior of K438G superalloy at 1000°C. Journal of the European Ceramic Society, 2017, 37, 1013-1022.	5.7	10
42	High vacuum arc ion plating TiAl coatings for protecting titanium alloy against oxidation at medium high temperatures. Corrosion Science, 2016, 112, 36-43.	6.6	26
43	Synthesis of advanced aluminide intermetallic coatings by low-energy Al-ion radiation. Scientific Reports, 2016, 6, 26535.	3.3	5
44	Effects of surface finish of single crystal superalloy substrate on cyclic thermal oxidation of its nanocrystalline coating. Corrosion Science, 2016, 111, 313-324.	6.6	26
45	TEM study of the evolution of sputtered Ni+CrAlYSiHfN nanocomposite coating with an AlN diffusion barrier at high temperature. Surface and Coatings Technology, 2016, 286, 262-267.	4.8	15
46	Microstructure and oxidation behavior of a Ni+CrAlYSiHfN/AlN multilayer coating fabricated by reactive magnetron sputtering. Corrosion Science, 2016, 104, 197-206.	6.6	18
47	The effect of yttrium addition on oxidation of a sputtered nanocrystalline coating with moderate amount of tantalum in composition. Applied Surface Science, 2016, 366, 245-253.	6.1	44
48	A duplex nanocrystalline coating for high-temperature applications on single-crystal superalloy. Corrosion Science, 2016, 102, 72-83.	6.6	27
49	Effect of sand blasting on oxidation behavior of K38G superalloy at 1000°C. Corrosion Science, 2015, 92, 256-262.	6.6	21
50	High vacuum arc ion plating NiCrAlY coatings: Microstructure and oxidation behavior. Corrosion Science, 2015, 94, 294-304.	6.6	71
51	Microstructure stabilization of a novel glass/YSZ composite coating material by adding alumina particles. Ceramics International, 2015, 41, 9753-9762.	4.8	11
52	Spontaneous reaction formation of Cr23C6 diffusion barrier layer between nanocrystalline MCrAlY coating and Ni-base superalloy at high temperature. Corrosion Science, 2015, 99, 219-226.	6.6	24
53	Influences of MCrAlY coatings on oxidation resistance of single crystal superalloy DD98M and their inter-diffusion behaviors. Journal of Alloys and Compounds, 2015, 649, 515-530.	5.5	55
54	Comparative study of oxidation and interdiffusion behavior of AIP NiCrAlY and sputtered nanocrystalline coatings on a nickel-based single-crystal superalloy. Corrosion Science, 2015, 98, 530-540.	6.6	70

#	Article	IF	CITATIONS
55	Oxidation behavior of glass-based composite thermal barrier coating on K417G superalloy with a NiCoCrAlY bond coat at 1000°C. Surface and Coatings Technology, 2015, 270, 314-323.	4.8	11
56	Yttria partially stabilised zirconia as diffusion barrier between NiCrAlY and Ni-base single crystal René N5 superalloy. Corrosion Science, 2015, 94, 122-128.	6.6	49
57	Ta effect on oxidation of a nickel-based single-crystal superalloy and its sputtered nanocrystalline coating at 900–1100 °C. Applied Surface Science, 2015, 345, 194-203.	6.1	64
58	High temperature oxidation of NiCrAlY, nanocrystalline and enamel-metal nano-composite coatings under thermal shock. Corrosion Science, 2015, 100, 556-565.	6.6	31
59	Microstructural stability of AlN diffusion barrier for nanocomposite Ni + CrAlYSiHfN coating on single crystal superalloy at high temperatures. Applied Surface Science, 2015, 359, 420-425.	6.1	13
60	High vacuum arc ion plating NiCrAlY coatings: Bias effect and approach to preparation of functional gradient coatings. Surface and Coatings Technology, 2015, 281, 44-50.	4.8	24
61	Characterization and Oxidation Behavior of a Sputtered Nanocomposite Ni+CrAlYSiHfN Coating. Corrosion, 2015, 71, 523-535.	1.1	16
62	A magnetron sputtered microcrystalline β-NiAl coating for SC superalloys. Part I. Characterization and comparison of isothermal oxidation behavior at 1100ŰC with a NiCrAlY coating. Applied Surface Science, 2015, 324, 1-12.	6.1	38
63	Development of an oxidation resistant glass–ceramic composite coating on Ti–47Al–2Cr–2Nb alloy. Applied Surface Science, 2014, 292, 583-590.	6.1	26
64	Microstructure and oxidation behavior of a SiC–Al2O3–glass composite coating on Ti–47Al–2Cr–2Nb alloy. Corrosion Science, 2014, 87, 179-186.	6.6	34
65	Glass coatings on stainless steels for high-temperature oxidation protection: Mechanisms. Corrosion Science, 2014, 82, 316-327.	6.6	57
66	Influence of Sputtered Nanocrystalline Coating on Oxidation and Hot Corrosion of a Nickel-based Superalloy M951. Journal of Materials Science and Technology, 2014, 30, 867-877.	10.7	42
67	Comparison of the cyclic oxidation behavior of a low expansion Ni+CrAlYSiN nanocomposite and a NiCrAlYSi coating. Corrosion Science, 2014, 80, 393-401.	6.6	30
68	Thermophysical Properties of Alumina Particle Reinforced Glass Matrix Composites. International Journal of Applied Ceramic Technology, 2013, 10, 224-233.	2.1	18
69	Glass–ceramic coatings on titanium alloys for high temperature oxidation protection: Oxidation kinetics and microstructure. Corrosion Science, 2013, 74, 178-186.	6.6	59
70	Interfacial reactions between a SiO2Al2O3ZnOCaO based glass and alpha alumina. Surface and Coatings Technology, 2013, 232, 6-12.	4.8	13
71	Strengthening mechanisms and fracture surface characteristics of silicate glass matrix composites with inclusion of alumina particles of different particle sizes. Physica B: Condensed Matter, 2013, 413, 15-20.	2.7	21
72	SiO2–Al2O3–glass composite coating on Ti–6Al–4V alloy: Oxidation and interfacial reaction behavior. Corrosion Science, 2013, 74, 367-378.	6.6	71

#	Article	IF	CITATIONS
73	Hot corrosion behaviour of a Ni+CrAlYSiN composite coating in Na2SO4–25wt.% NaCl melt. Applied Surface Science, 2013, 268, 103-110.	6.1	42
74	Comparative study of interfacial reaction between superalloy substrate and glass coating with and without alumina particles incorporation. Applied Surface Science, 2013, 271, 228-233.	6.1	21
75	Effect of sand blasting and glass matrix composite coating on oxidation resistance of a nickel-based superalloy at 1000 ŰC. Corrosion Science, 2013, 73, 331-341.	6.6	36
76	Phase Evolution of <scp><scp>SiO</scp></scp> <sub>2</sub> – <scp><scp>Al</scp></scp> <sub>2</sub> <scp>O</scp> Glass with Added Yâ€ <scp>PSZ</scp> Particles. Journal of the American Ceramic Society, 2013, 96, 1456-1463.	scp> <sub: 3.8</sub: 	>3–∢ 15
77	Oxidation and Thermal Shock Behavior of a Glass-Alumina Composite Coating on K38G Superalloy at 1000 °C. Journal of Materials Science and Technology, 2012, 28, 433-438.	10.7	21
78	The scaling behavior of sputtered Ni3Al coatings with and without Pt modification. Corrosion Science, 2012, 58, 115-120.	6.6	25
79	Preparation and oxidation behaviour of nanocrystalline Ni+CrAlYSiN composite coating with AlN diffusion barrier on Ni-based superalloy K417. Corrosion Science, 2012, 60, 265-274.	6.6	54
80	Preparation and thermal shock behavior at 1000°C of a glass-alumina-NiCrAlY tri-composite coating on K38G superalloy. Surface and Coatings Technology, 2012, 206, 2566-2571.	4.8	25
81	Glass–alumina composite coatings for high temperature corrosion protection. Part I: Effect of crystallization and interfacial reaction on the thermo-physical properties. Materials Science & Engineering A: Structural Materials: Properties, Microstructure and Processing, 2011, 528, 3186-3192.	5.6	19
82	Effect of NiCrAlY platelets inclusion on the mechanical and thermal shock properties of glass matrix composites. Materials Science & Engineering A: Structural Materials: Properties, Microstructure and Processing, 2011, 528, 1360-1366.	5.6	27
83	High temperature corrosion behavior of an AIP NiCoCrAlY coating modified by aluminizing. Surface and Coatings Technology, 2011, 205, 5053-5058.	4.8	39
84	Cyclic oxidation behavior of glass–ceramic composite coatings on superalloy K38G at 1100°C. Thin Solid Films, 2011, 519, 4884-4888.	1.8	16
85	Crystallization Behavior of SiO <sub>2</sub> –Al <sub>2</sub> O <sub>3</sub> –ZnO–CaO Glass System at 1123–1273 K. Journal of the American Ceramic Society, 2010, 93, 3230-3235.	3.8	34
86	Effect of vitreous enamel coating on the oxidation behavior of Ti6Al4V and TiAl alloys at high temperatures. Journal of Coatings Technology Research, 2008, 5, 93-98.	2.5	22
87	Electronic Structure of Monomeric Water Adsorption on Ni{111}: Beyond the General Model. Journal of Physical Chemistry C, 2008, 112, 8301-8303.	3.1	11
88	Synergistic corrosion behavior of coated Ti60 alloys with NaCl deposit in moist air at elevated temperature. Corrosion Science, 2008, 50, 15-22.	6.6	46
89	Amorphous sol–gel SiO2 film for protection of Ti6Al4V alloy against high temperature oxidation. Surface and Coatings Technology, 2007, 201, 5967-5972.	4.8	42
90	The effect of yttrium addition on the isothermal oxidation behavior of sputtered K38 nanocrystalline coating at 1273ÂK in air. Surface and Coatings Technology, 2007, 201, 7425-7431.	4.8	27

#	Article	IF	CITATIONS
91	Oxidation and hot corrosion behavior of a novel enamel-Al2O3 composite coating on K38G superalloy. Surface and Coatings Technology, 2006, 200, 5931-5936.	4.8	53
92	The oxidation behavior and mechanical performance of Ti60 alloy with enamel coating. Surface and Coatings Technology, 2005, 190, 195-199.	4.8	67
93	Influence of columnar microstructure of a sputtered NiAl coating on its oxidation behavior at 1000°C. Intermetallics, 2002, 10, 467-471.	3.9	46
94	The mechanism of scale adhesion on sputtered microcrystallized CoCrAl films. Oxidation of Metals, 1996, 45, 39-50.	2.1	63
95	Reactive sputter deposition of alumina films on superalloys and their high-temperature corrosion resistance. Surface and Coatings Technology, 1995, 71, 9-15.	4.8	68
96	Rehealing ability of oxide scales formed on microcrystalline K38G coatings. Oxidation of Metals, 1995, 43, 317-328.	2.1	45